

Angle-resolved photoelectron spectroscopy of the nickel magnetism below and above T_C

Autor(en): **Gerhard, Ulrich**

Objektyp: **Article**

Zeitschrift: **Helvetica Physica Acta**

Band (Jahr): **56 (1983)**

Heft 1-3

PDF erstellt am: **08.08.2024**

Persistenter Link: <https://doi.org/10.5169/seals-115363>

Nutzungsbedingungen

Die ETH-Bibliothek ist Anbieterin der digitalisierten Zeitschriften. Sie besitzt keine Urheberrechte an den Inhalten der Zeitschriften. Die Rechte liegen in der Regel bei den Herausgebern.

Die auf der Plattform e-periodica veröffentlichten Dokumente stehen für nicht-kommerzielle Zwecke in Lehre und Forschung sowie für die private Nutzung frei zur Verfügung. Einzelne Dateien oder Ausdrucke aus diesem Angebot können zusammen mit diesen Nutzungsbedingungen und den korrekten Herkunftsbezeichnungen weitergegeben werden.

Das Veröffentlichen von Bildern in Print- und Online-Publikationen ist nur mit vorheriger Genehmigung der Rechteinhaber erlaubt. Die systematische Speicherung von Teilen des elektronischen Angebots auf anderen Servern bedarf ebenfalls des schriftlichen Einverständnisses der Rechteinhaber.

Haftungsausschluss

Alle Angaben erfolgen ohne Gewähr für Vollständigkeit oder Richtigkeit. Es wird keine Haftung übernommen für Schäden durch die Verwendung von Informationen aus diesem Online-Angebot oder durch das Fehlen von Informationen. Dies gilt auch für Inhalte Dritter, die über dieses Angebot zugänglich sind.

ANGLE-RESOLVED PHOTOELECTRON SPECTROSCOPY
OF THE NICKEL MAGNETISM BELOW AND ABOVE T_c

Ulrich Gerhard

Physikalisches Institut der Universität
Robert-Mayer-Strasse 2-4, D-6000 Frankfurt am Main

The basic quantity of the Stoner model designed to explain the itinerant electron ferromagnetism of the transition metals is the exchange splitting Δ_x . It is sobering to note that more than 40 years had to pass since this model was introduced by Slater and Stoner before Δ_x could be identified experimentally. The main difficulty which prevented earlier detection arises from the fact that methods like optical or angle-integrated photoelectron spectroscopy average over the contributions of the various 3d-components, thus swamping the minor modification introduced by the exchange splitting. Only after isolating one single component of the 3d-band close to the Fermi energy E_F by angle resolved ultraviolet photoelectron spectroscopy (ARUPS) could its exchange splitting be detected. ⁽¹⁾

The method is illustrated in Fig. 1, which shows schematically the dispersion of the final band and of the one 3d-component close to E_F along the $[11\bar{2}]$ and $[\bar{1}\bar{1}2]$ directions perpendicular to the Δ axis, i.e. tangential to the (111) surface of the sample. The 3d-component consists actually of the majority and the minority subband separated by the exchange splitting.

The one 3d-component close to E_F which is shown in Fig. 1 is singled out by considering the dipol matrix elements of the direct optical transitions which might possibly contribute to the photoemission in this geometry. For light polarized

perpendicular to $(1\bar{1}0)$, only the two components with odd parity with respect to the $(1\bar{1}0)$ mirror reflection may contribute since the dipole matrix elements of the remaining three even parity components are zero by symmetry. ⁽²⁾ For photon energies ω below 13.5 eV, only the odd parity component close to E_F contributes significantly to photoemission in the $[\bar{1}\bar{1}2]$ azimuth; it still dominates the photoemission for small polar angles in the $[1\bar{1}\bar{2}]$ azimuth. ^(3,4)

The azimuthal and polar angles of detection and the photon energy ω determine the k_t value at which the 3d subbands shown in Fig. 1 are sampled by the corresponding photoelectron spectra. In the upper part of Fig. 1, two such spectra taken

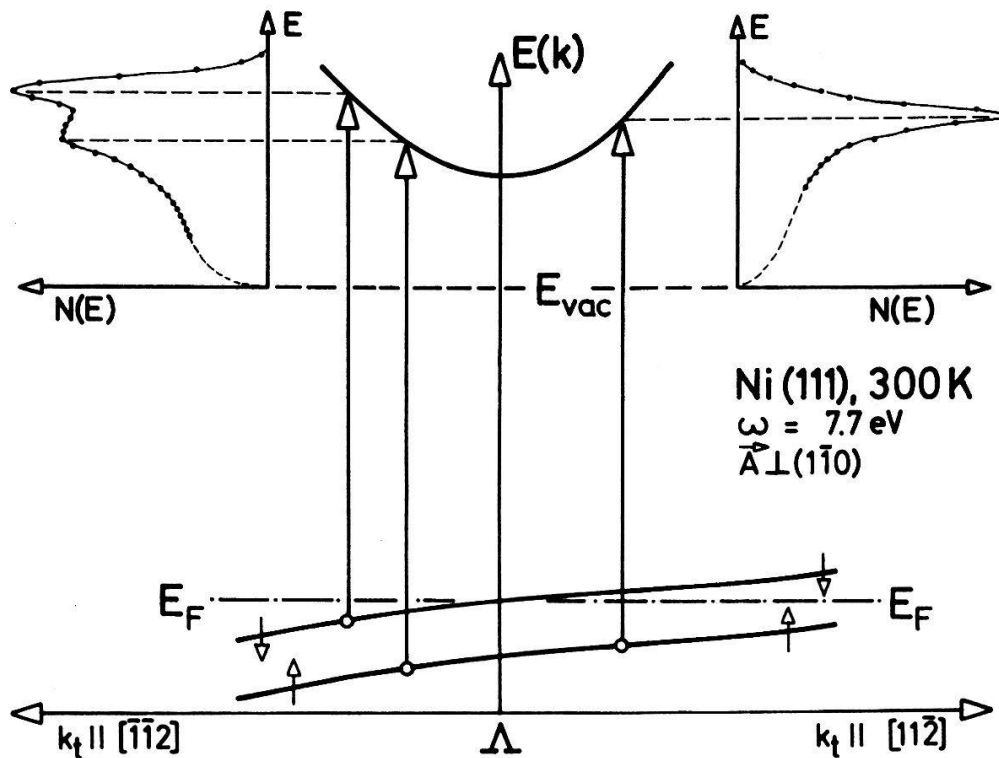


Fig. 1: Schematic dispersion of the final band and of the two initial subbands originating from one 3d-component, together with two measured photoelectron spectra for a polar angle of 45° .

recently for 300 K, $\omega = 7.7$ eV and a polar angle of 45° are given. The $[\bar{1}\bar{1}2]$ spectrum does indeed show the expected doublet structure caused by Δ_x , while only one peak is observed for the $[11\bar{2}]$ azimuth since the minority subband lies above E_F in this case. The observed dispersion of the 3d-component is in agreement with the one calculated selfconsistently ⁽⁵⁾ and also with the dispersion of the corresponding component in Cu. ⁽³⁾ The same behaviour was found in the $\omega = 10.2$ eV spectra where the exchange doublet was first identified. ⁽¹⁾ These results were later confirmed by two different groups. ^(6,7,8)

The discussion so far assumed contributions from bulk states only. This assumption is justified since the (111) surface state of Ni which interferes for normal emission ⁽⁷⁾ does not contribute to the off normal spectra of Fig. 1. The results are however drastically modified by the self-energy corrections to the final state, caused by the correlations among the 3d electrons. ⁽⁹⁾ The two effects most important for the present discussion are the strong increase of the observed peak width with binding energy, which is apparent in the $[\bar{1}\bar{1}2]$ spectrum of Fig. 1, and the strong decrease of the measured Δ_x ⁽¹⁰⁾ as compared to Δ_x calculated selfconsistently for the ground state. ⁽⁵⁾

The experimental identification of Δ_x at room temperature where the saturation magnetization M_s is already quite close to $M_{s0} = M_s(T = 0 \text{ K})$ certainly supports the validity of the Stoner model in the ground state. Additional support comes from room temperature ARUPS taken at normal emission from a Ni (110) surface. ⁽¹¹⁾ The situation is more complex in this case since two 3d-components overlap, each showing an exchange splitting. The original assignment ⁽¹¹⁾ was recently confirmed by measuring the spin polarization of the emitted photoelectrons in addition to their angle-resolved energy distribution. ⁽¹²⁾

At higher temperatures, however, the Stoner model is in contradiction with a variety of observations, the most prominent of which are the large magnitude of the observed ⁽¹⁰⁾ and calculated ⁽⁵⁾ exchange splitting which is about five and ten times kT_c (the thermal energy at the Curie temperature), respectively, and the observation of spin waves well above T_c in neutron scattering experiments. ⁽¹³⁾ The work of Eastman, Himpsel, and Knapp ⁽⁶⁾ on the temperature dependence of the Ni (111) exchange doublet added another contradiction: They determined the exchange splitting by a least squares fit to a superposition of two Lorentzians and a background and found that the exchange splitting does not vanish above T_c . We have confirmed their results by performing a least squares fit to our spectra more recently obtained with high energy and angular resolution (40 meV and 2.8° full width at half maximum),

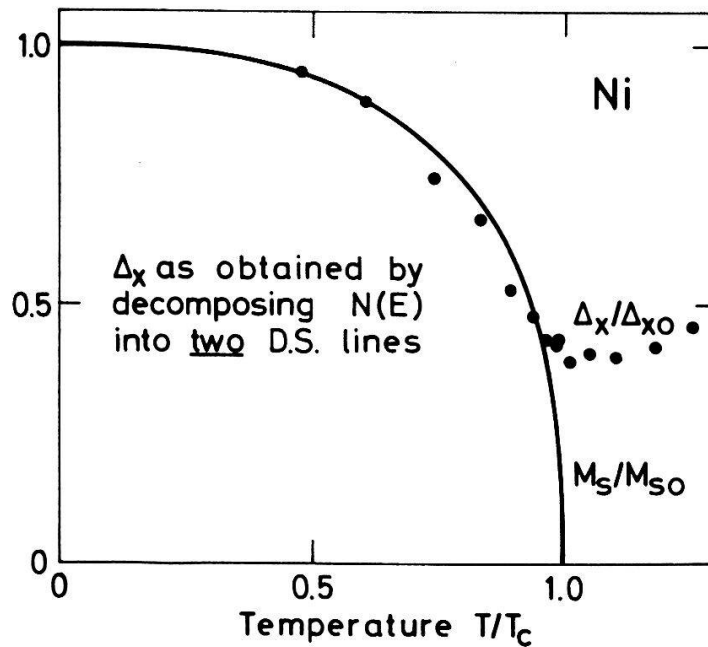


Fig. 2 : Temperature variation of the saturation magnetization M_s and of the exchange splitting Δ_x . The exchange splitting is normalized to M_s at room temperature.

superimposing two Doniach-Sunjic (DS) lines. ⁽¹⁰⁾ In this approach, the asymmetry of the lines is not described by a background but more physically by the additional excitation of many low energy electron-hole pairs. ⁽¹⁴⁾ Our result is given in Fig.2, which also shows the saturation magnetization $M_s(T)$.

In order to reconcile the magnetic properties of Ni at high temperatures with theory, Korenman, Murray, and Prange ⁽¹⁵⁾ and Capellmann ⁽¹⁶⁾ developed the local band or short range magnetic order (SRMO) model. They assume essentially no change of the exchange splitting with temperature where this quantity is now defined locally. The decrease in M_s with temperature is now accounted for by an increase in the transverse fluctuations of the spin density vector which eventually destroy the long range magnetic order above T_c while the SRMO persists on a scale of about 20 \AA . Korenman and Prange also estimated the ARUPS line shape at elevated temperatures: ⁽¹⁷⁾ It should consist of the two magnetic lines F_{\uparrow} and F_{\downarrow} with essentially unchanged separation Δ_x but decreased intensity and a nonmagnetic line F_0 between them in addition. The line F_0 corresponds to scattering of the photoelectrons by the transverse fluctuations of the spin density vector. The intensity of this nonmagnetic line should thus increase while its width ought to decrease with temperature ("motional narrowing").

The predictions of the SRMO model can be tested by ARUPS since it is a local probe: Without analysing the spin polarization, the photoelectrons carry information about the magnetic configuration within a volume of about L^3 , where L is the escape depth of the photoelectrons which is roughly

20 Å for $\omega = 7.7$ eV. (18,19) For example, the low temperature exchange doublet will be observed even if the magnetization gradually changes its direction on a larger scale given by the lateral coherence length l_c but is essentially homogeneous within L^3 . This coherence length is mainly given by the angular resolution $\Delta\vartheta_0$, namely $\vec{l}_c \cdot \vec{\Delta k}_0 \approx \pi$ and $\Delta\vartheta_0 \approx \Delta k_0/k_0$, where k_0 is the wave vector in vacuum. For the spectra discussed here, $l_c \approx 10L$.

We incorporate the three peak structure predicted by Korenman and Prange by equating the two magnetic components F_{\uparrow} and F_{\downarrow} with the two DS lines obtained from the room temperature fit. These two lines are given in the lower part of Fig. 3, which also shows the exchange doublet for $\omega = 7.7$ eV at 300 K (rectangles) and the superposition of the two DS lines fitting the doublet (fine dots). For higher temperatures, the third nonmagnetic line F_0 is added, again using the DS form. The energy position, width, and fractional intensity of F_0 are treated as adjustable parameters in the least squares fit. One example of this three peak fit is shown at $T = 1.01T_c$ in the upper part of Fig. 3. The Fig. 5 presents the temperature variation of the fractional intensity η_0 and of the width $2\gamma_0$ for the nonmagnetic peak F_0 , extracted from similar three peak fits to the photoelektron spectra taken at various temperatures. The predictions of the SRMO model are indeed borne out by the experimental results: The fractional intensity of F_0 increases and, most significantly, its width $2\gamma_0$ decreases with increasing temperature, thus strongly supporting the SRMO model.

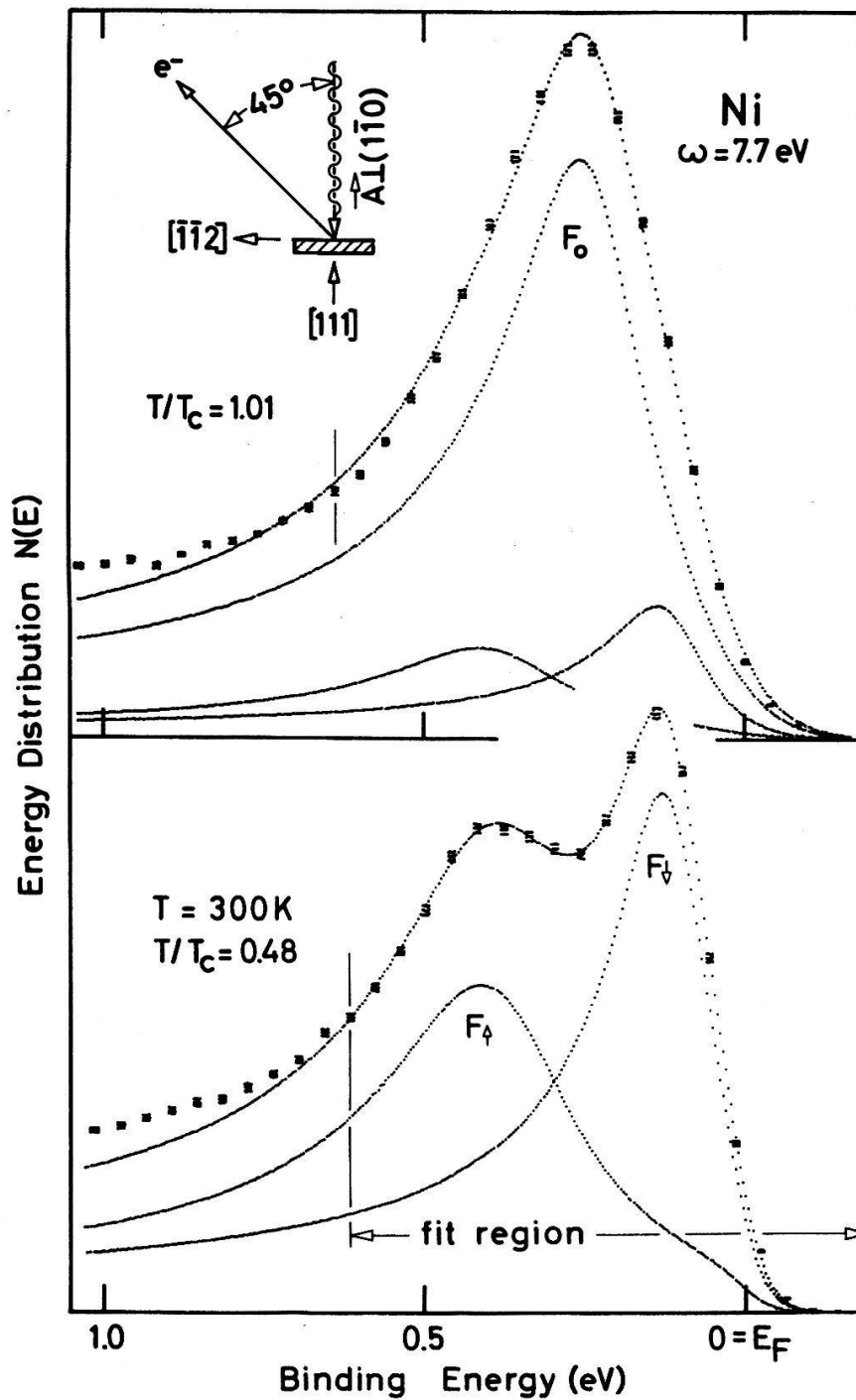


Fig. 3: The Ni(111) spectra, taken in the $[\bar{1}\bar{1}2]$ azimuth under 45° with $\omega = 7.7 \text{ eV}$ and the light polarized perpendicular to $(1\bar{1}0)$. the height of the rectangles is twice the statistical error. Fine dots refer to fit.

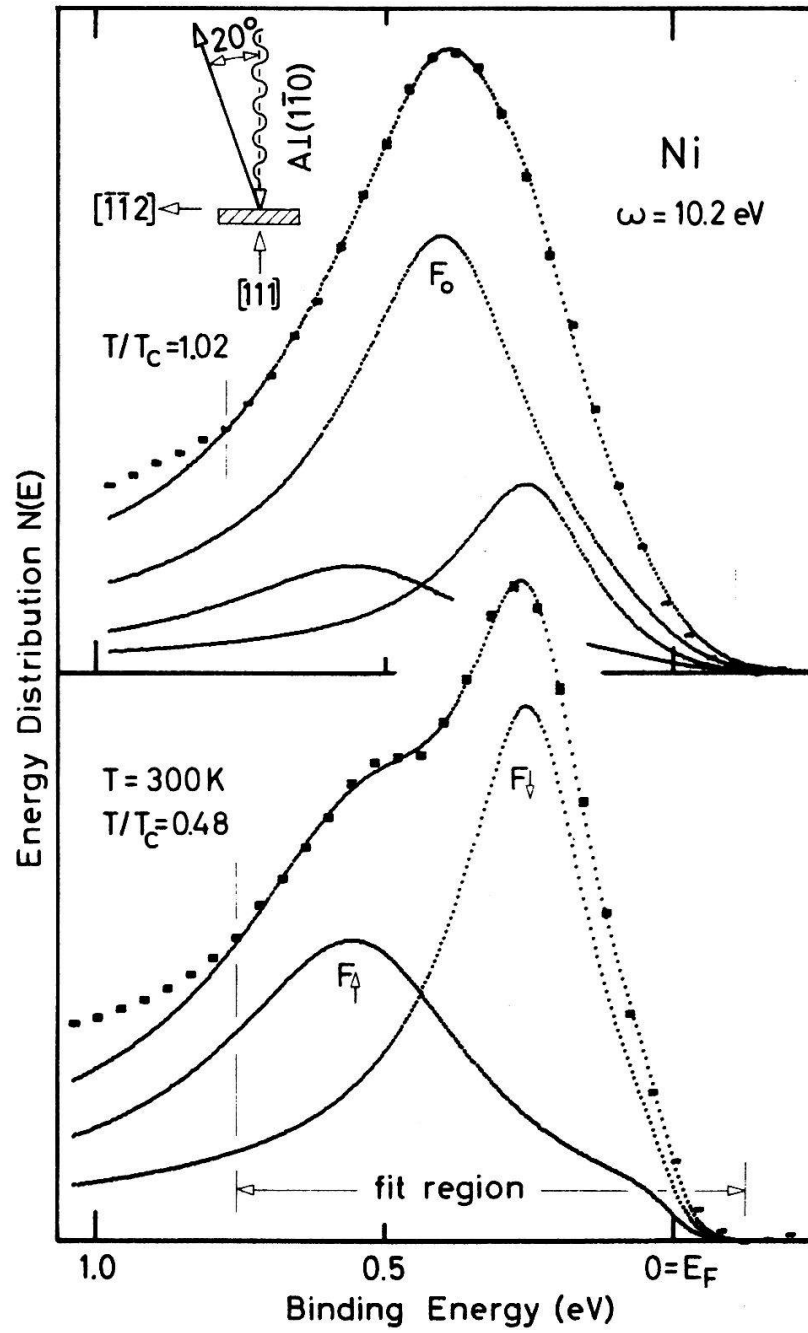


Fig. 4: The Ni(111) spectra as in Fig. 3 except for $\omega = 10.2$ eV and a polar angle of 20° .

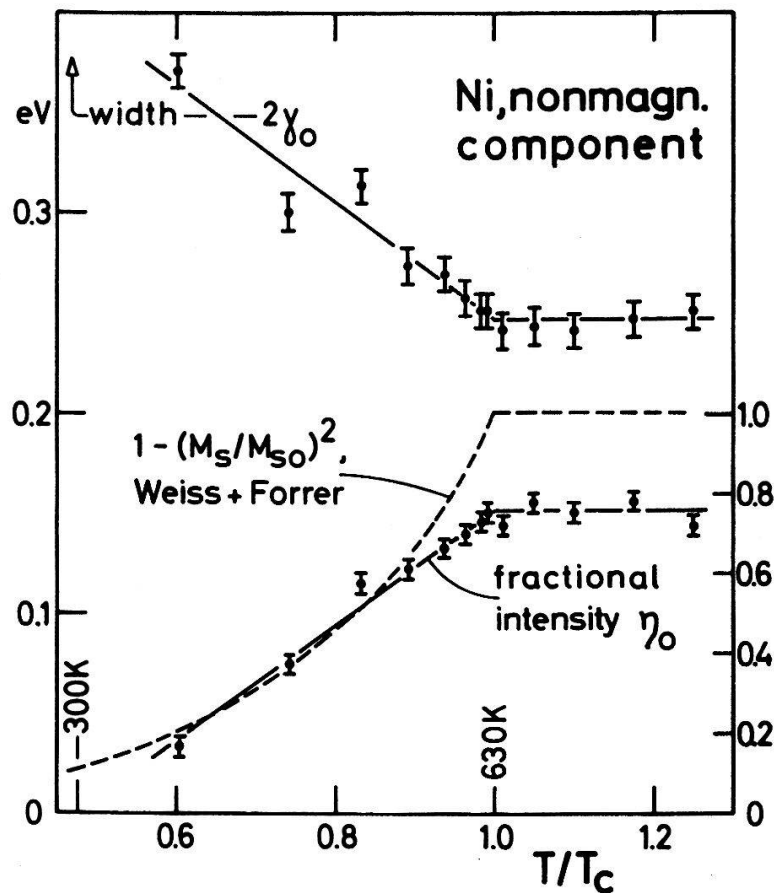


Fig. 5: Fractional intensity and width of the nonmagnetic peak F_0 , evaluated for the $\omega = 7.7$ eV spectra.

The escape depth of the photoelectrons depend on their energy. For $\omega = 10.2$ eV it has decreased to about 12 \AA . (18,19) This decrease in L corresponds to an additional uncertainty in the wave vector component normal to the surface and thus to a broadening of the spectra. This is readily observed: The room temperature doublet at $\omega = 10.2$ eV (lower part of Fig. 4) is not as well resolved as the corresponding $\omega = 7.7$ eV doublet (lower part of Fig. 3). On the other hand, for high but fixed temperatures a decrease in L should mean that the corresponding photoelectrons experience a more homo-

geneous magnetization. The SRMO model predicts therefore a higher fractional intensity of the magnetic lines above T_c for $\omega = 10.2$ eV as compared to $\omega = 7.7$ eV, an effect which is again clearly observed by comparing the three peak decomposition given in the upper panel of Fig. 4 with the corresponding panel of Fig. 3. In fact the contribution of the minority peak to the $T = 1.02T_c$, $\omega = 10.2$ eV spectrum of Fig. 4 is easily identified visually as the shoulder at a binding energy of 0.25 eV without even performing a least squares fit! The three peak analysis thus confirms the predictions of the SRMO model in every detail, which is surprising as well as reassuring since the model was first designed to explain the existence of spin waves well above T_c as observed in neutron scattering experiments.

The results presented in this paper were obtained by a team which consists of or has formerly included E. Dietz, R. J. Jelitto, C. J. Maetz, A. Scheidt, A. Schütz, J. Würtenberg, A. Ziegler, and myself. I thank them all for the privilege of being able to present the results of our joint venture. I also acknowledge valuable discussions with H. Capellmann, V. Korenman, and R. Prange.

- 1) E. Dietz, U. Gerhardt, and C. J. Maetz, Phys. Rev. Lett. 40, 892 (1978)
- 2) J. Hermanson, Solid State Comm. 22, 9 (1977)
- 3) E. Dietz and U. Gerhardt, J. Phys. F 8, 2213 (1978)
- 4) E. Dietz and D. E. Eastman, Phys. Rev. Lett. 41, 1674 (1978)
- 5) C. S. Wang and J. Callaway, Phys. Rev. B 15, 298 (1977)
- 6) D. E. Eastman, F. J. Himpsel, and J. A. Knapp, Phys. Rev. Lett. 40, 1514 (1978)
- 7) F. J. Himpsel, J. A. Knapp, and D. E. Eastman, Phys. Rev. B 19, 2919 (1979)
- 8) P. Heimann and H. Neddermeyer, J. Magn. Magn. Mater. 15-18 1143 (1980)
- 9) A. Liebsch, Phys. Rev. Lett. 43 1431 (1979)
- 10) C. J. Maetz, U. Gerhardt, E. Dietz, A. Ziegler, and R. J. Jelitto, Phys. Rev. Lett. 48, 1686 (1982)
- 11) P. Heimann, F. J. Himpsel, and D. E. Eastman, Solid State Comm. 39, 219 (1981)
- 12) R. Raue, H. Hopster, and R. Clauberg, to be published
- 13) J. W. Lynn and H. A. Mook, Phys. Rev. B 23, 198 (1981)
- 14) S. Doniach and M. Šunjić, J. Phys. C 3, 285 (1970)

- 15) V. Korenman, J. Murray, and R. Prange, Phys. Rev. B 16, 4032, 4048, 4058 (1977) and 19, 4691, 4698 (1979)
- 16) H. Capellmann, Z. Phys. B 34, 29 (1979) and 35, 269 (1979)
- 17) V. Korenman and R. E. Prange, Phys. Rev. Lett. 44, 1291 (1980)
- 18) D. E. Eastman, Solid State Comm. 8, 41 (1970)
- 19) J. W. T. Ridgeway and D. Haneman, Surf. Sci. 24, 451 (1971)